ingegneria sismica
International Journal of Earthquake Engineering
Anno XLIII - Num. 3 - 2026

Temperature measurement of automobile engine based on various thermocouples

You Zhou[1], *Bowen Deng*[1], *Dongfen Li*[1,*], *Wentao Ni*[1], *Yixuan Huang*[1], *Weiqian Liang*[1] *and Jianyuan Tang*[1]

[1] Chengdu University of Technology, College of Computer and Network Security, 1#, Dongsanlu, Erxianqiao, Chengdu 610059, Sichuan, P.R.China

SUMMARY: *With the rapid development of the automobile industry, numerous accidents caused by vehicle spontaneous combustion due to excessive engine temperatures have raised widespread concerns in society. Therefore, this paper proposes a high-precision temperature measurement method based on various thermocouples. Firstly, one end of K/T/E-type thermocouples is attached to the outer surface of a constant temperature oil tank. The corresponding voltage and temperature values are recorded every 30 minutes as the temperature of the oil tank increases, and a voltage-temperature curve is plotted. The Seebeck coefficient of the K-type thermocouple is 41.55 μV/°C, the Seebeck coefficient of the T-type thermocouple is 38.84 μV/°C, and the Seebeck coefficient of the E-type thermocouple is 57 μV/°C. Subsequently, the thermocouples are applied to the surface of the automobile engine, and the multimeter readings are continuously recorded after the engine is started. Based on the Seebeck coefficients of the thermocouples, the temperature of the GG-K-30 K-type thermocouple rises rapidly from approximately 12°C to 80°C within 0.5-4.5 minutes, further increasing to around 120°C within 4.5-9.5 minutes, and then stabilizing at approximately 122°C. The temperature of the TT-K-30 K-type thermocouple rises from about 7°C to 75°C within 0.5-4.5 minutes, reaching approximately 120°C within 4.5-10 minutes, and then stabilizes at about 124°C. The temperature of the T-type thermocouple increases from around 12°C to 80°C within 0.5-5 minutes, rises to about 120°C within 4.5-9.5 minutes, and then stabilizes at around 123°C. The temperature of the E-type thermocouple with a length of 2000 mm rises from around 8°C to 86°C within 0.5-6.5 minutes, further increasing to 120°C within 6.5-10.5 minutes, and then stabilizing at about 122°C. The temperature of the E-type thermocouple with a length of 1000 mm rises from approximately 5°C to 75°C in 0.5-5.5 minutes, reaching 120°C in 5.5-10 minutes, and then stabilizing at about 121°C. Experiments show that the thermocouple temperature measurement method has good accuracy and stability, allowing for real-time continuous measurement of engine temperature and providing danger warnings. This method offers an effective and reliable solution to the temperature-related issues of automobile engines.*

KEYWORDS: *temperature, thermocouple, Zeebek coefficient, static calibration, automobile engine*

1 Introduction

As one of the fundamental physical quantities, temperature is a crucial characteristic in fields

*zhouyou202504@163.com
https://doi.org/10.65102/is20261186
Published: 10 June, 2026

such as human physiology, agriculture, and industrial manufacturing. It not only directly reflects the thermal properties of the measured object but also provides a basis for judging other characteristics [1-3]. Currently, the most commonly used temperature measurement method is non-contact temperature measurement (e.g., spectral radiation and infrared thermal imaging), which is based on the blackbody radiation law [4, 5]. However, with the continuous advancement of modern science and technology, the accuracy of non-contact temperature measurements has been found to be relatively low. Improving the accuracy and efficiency of these measurements has become a significant challenge for scientists, which is why finding a more efficient temperature measurement method has been discussed at various international summits in recent years [6].

For instance, at the 27th China Process Control Conference in 2016, Pan Dong proposed using thermocouple data to overcome the harsh environment at blast furnace sites, aiming to address the issues of short equipment lifespans and low measurement accuracy in monitoring the temperature of molten iron in the main ditch of the blast furnace. This provided a new method for detecting the temperature of molten iron [7]. Additionally, Li Zhenwei introduced a K-type (NiCr/NiSi) thin-film thermocouple at the third International Conference on Electromechanical Control Technology and Transportation in 2018. Through extensive experimentation, it was demonstrated that thin-film thermocouples have shorter response times and smaller relative errors than traditional thermocouples [8].

These studies highlight the increasing importance of thermocouples in temperature measurement, making it a key topic in sensor technology. This article aims to use T-type, K-type, and E-type thermocouples to collect temperature data, in order to promote innovative development of temperature measurement technology. The advantages of this approach include: first, thermocouples improve measurement accuracy and broaden the temperature range. While the upper temperature limit of common thermometers is usually around 480°C, thermocouples can reach temperatures as high as 1500°C [9]. Second, thermocouples do not require an external power supply, as they measure temperature by dividing the voltage value by the Seebeck coefficient of the thermocouple, which is beneficial for environmental protection [10, 11]. Third, thermocouples possess excellent anti-interference capabilities. The tiny voltage signal they generate is not easily disturbed by electromagnetic fields and other external factors, which is critical for industrial temperature measurements [12, 13].

Traditionally, temperature collection is often non-contact. For example, Li Peng and others studied the operation monitoring of rural distribution network equipment using infrared temperature measurement technology [14]. The false detection rate of the monitoring results was only 3.70%, indicating that infrared temperature measurement technology has significant potential in the operation monitoring of power equipment. Reference [15] used an infrared thermal imager to analyze how emissivity affects temperature measurement accuracy. The results showed that when the emissivity was 0.7, the real temperature was 50°C, and when the emissivity deviated by 0.1, the temperature measurement error ranged from 0.76 to 0.89°C for a 3-5 μm thermal imager. For an 8-14 μm thermal imager, the error was between 1.56°C and 1.87°C. Reference [16] used the dual color planar laser-induced fluorescence technique of OH hydroxyl radicals, combined with the coherent anti Stokes Raman scattering spectroscopy method of H_2 molecules, to measure the temperature of methane combustion flames in air, and successfully obtained temperature field distribution data in the core area of methane flames. Reference [17] used interferometric thermometry to demonstrate that after a 20ms laser pulse, the temperature uncertainty was 0.9°C, with peak heating around 17°C. This method is expected to be used for the calibration of non-invasive retinal laser therapy.

Although the methods discussed above offer effective and convenient temperature measurement techniques, they still face issues such as limited measurement range, low

accuracy, and interference from external factors. This makes it difficult to ensure the accuracy of experimental results and the consistency of results across different environments. As a result, these research methods are limited in their application and cannot provide accurate temperature measurements in a variety of settings, particularly for high-temperature applications. Given the instability in traditional technology, many researchers still face significant errors in their experimental temperature measurements, which can greatly affect the conclusions of their experiments. Therefore, there is a need to explore a more accurate and reliable temperature measurement method that can ensure long-term precision and broaden the measurable temperature range.

To address these issues, this paper refers to thermocouple technology. Initially, One end of the thermocouple is connected to the constant temperature oil tank to achieve corresponding connection and signal transmission functions. Then, the thermocouple is applied to the surface of the automobile engine, with the other end still connected to the multimeter. As the engine temperature rises, the corresponding voltage-time values are recorded and plotted as a graph. Finally, the temperature at each corresponding moment is calculated using the known Seebeck coefficient, enabling continuous and accurate engine temperature monitoring.

2 Principle of temperature sensor

The core of the temperature measurement mechanism of thin film thermocouples lies in the utilization of thermoelectric effects. In the specific experimental operation, two materials with different thermoelectric properties are selected to act as positive and negative electrodes, respectively, to construct a closed loop. Once a temperature difference is formed between the hot and cold ends, the heating of the hot node will trigger the Seebeck effect. This potential difference will cause a reverse current to be generated within the system until the dynamic equilibrium state of the electric field is reached. Ultimately, the system will output a stable thermoelectric potential [18-22]. The principle diagram of the temperature sensor is presented in Figure 1.

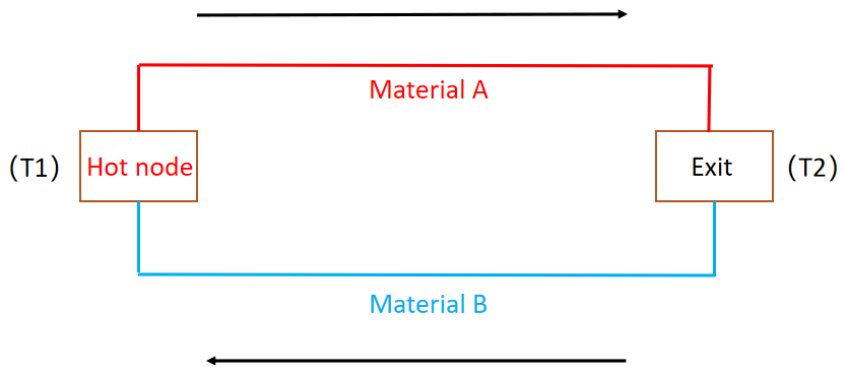

Figure 1: Thermoelectric effect principle

The calculation equation (1) of thermoelectromotive force is

$$E_{AB} = (S_A - S_B)(T_1 - T_2) = S_{AB}(T_1 - T_2) \quad (1)$$

Where, T_1 is the hot end temperature of the thin film thermocouple; E_{AB} is electromotive force output by the thin film thermocouple; T_2 is the cold end temperature of the thin film thermocouple; S_B is the Zeebek coefficient of material B; S_A is the Zeebek coefficient of material A.

3 Calibration experiments conducted under static conditions

3.1 Experimental setup

To establish the static calibration platform for thermocouple-based temperature measurement, a set of experimental apparatus was prepared, including an infrared thermometer, T-type, K-type, and E-type thermocouples, a digital multimeter, an alcohol lamp, industrial-grade high-temperature-resistant silicone oil, an iron support stand, asbestos mesh, and copper connecting wires.

During the setup process, a conical flask filled with industrial oil was placed centrally on an asbestos mesh supported by the iron frame to ensure uniform heating. The hot junctions of the T-type, K-type, and E-type thermocouples were affixed to the external wall of the conical flask at half the height of the liquid column using high-temperature-resistant adhesive tape to ensure consistent thermal contact. In practical operation, copper wire is used as an auxiliary medium to lead out the cold end of the thermocouple, and then the cold end is connected to the voltage input interface of a calibrated digital multimeter. During this process, it is necessary to ensure that the cold end of the thermocouple is always at room temperature to maintain a stable and uniform reference standard.

Before starting the heating process, it is necessary to use the function selection knob to set the multimeter to the DC voltage measurement mode, and select the measurement range as (0-20mV). The initial temperature of the silicone oil was measured using the infrared thermometer, and the corresponding voltage output was confirmed to be approximately 0 mV to establish a reliable baseline.

Subsequently, the alcohol lamp was ignited to serve as the heat source. The silicone oil within the conical flask was gradually heated, and both the temperature (via the infrared thermometer) and the corresponding thermoelectric voltage (via the multimeter) were recorded synchronously at 30-second intervals. This process continued until the temperature stabilized, indicating thermal equilibrium, at which point the heating source was extinguished and the multimeter powered off.

When the system temperature drops back to room temperature, perform the calibration process again to ensure good reproducibility of the experimental results. All recorded data were organized into a structured dataset. A two-dimensional coordinate graph was constructed, with thermoelectric voltage determined as the y-axis and temperature set as the x-axis. The thermoelectric behavior of each type of thermocouple was quantitatively analyzed by determining the slope of the linear fit, representing the Seebeck coefficient. Deviations from ideal linearity and experimental anomalies were carefully evaluated to assess potential sources of error, such as heat loss, delayed response of the sensor, imperfect thermal contact, or multimeter sensitivity limits. These analyses facilitated an objective evaluation of the accuracy and reliability of the thermocouple temperature measurements under controlled static conditions. Figure 2 shows the static calibration experimental platform diagram.

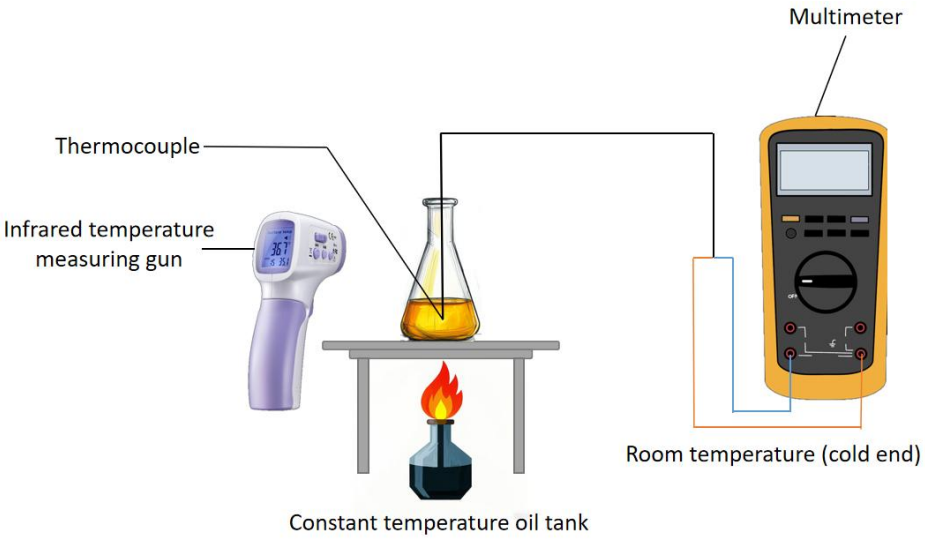

Figure 2: Static calibration experiment platform diagram

3.2 Analysis of experimental results

To reduce possible errors during the experimental process, after creating a stable constant temperature environment with the help of a constant temperature oil tank. After the successful completion of the experiment, a series of preprocessing tasks were carried out on the obtained data, including removing outliers and implementing standardized processing to improve the quality and accuracy of the experimental data.

3.2.1 Feasibility verification

The experimental results are shown in the following Figures 3~ Figures 5. Figure 3 shows the experimental data collected through a set of K-type thermocouples. The experimental data results shown in Figure 4 are matched with a single set of T-type thermocouples. And Figure 5 shows the experimental data related to a single set of E-type thermocouples.

The specific expression of the voltage temperature relationship equation (2) corresponding to the GG-K-30K thermocouple is as follows:

$$y=0.0411x-0.1776 \tag{2}$$

The correlation equation (3) between voltage and temperature corresponding to TT-K-30K thermocouple is as follows:

$$y=0.0414x-0.0697 \tag{3}$$

The Zeebek coefficient (i.e., the slope characteristic value) of K-type thermocouples is approximately 41.1 μ V/° C. As for the current situation, the Zeebek coefficient of K-type thermocouples is 41 μ V/° C according to the national standard. Therefore, it can be seen that the Zeebek coefficient value of K-type thermocouples obtained through this experiment is extremely close to the national standard value [23, 24].

Experimental measurements were conducted on the voltage temperature relationship expression (4) of T-type thermocouples, and the following results were obtained:

$$y=0.039x-0.5835 \tag{4}$$

Finally, experimental measurements were conducted on the voltage temperature relationship equation (5) corresponding to the E-type thermocouple with a length specification of 1000mm. The results are presented as follows [25, 26]:

$$y=0.0571x-0.2867 \quad (5)$$

The corresponding equation (6) between voltage and temperature for an E-type thermocouple with a length of 2000mm is as follows:

$$y=0.0567x-0.0814 \quad (6)$$

It can be reasonably inferred that the results of this experiment have a high degree of reliability, and it also indicates that the experimental equipment used is effective [27, 28].

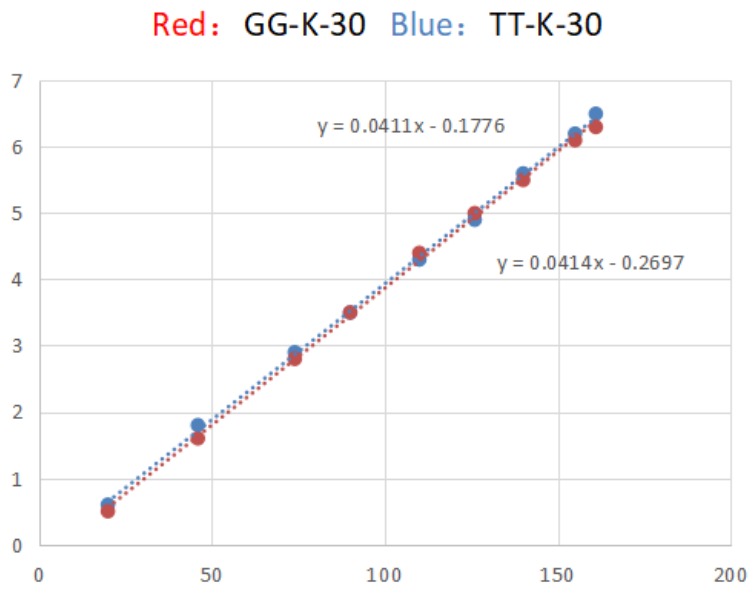

Figure 3: Single set experimental data chart (K-type thermocouple)

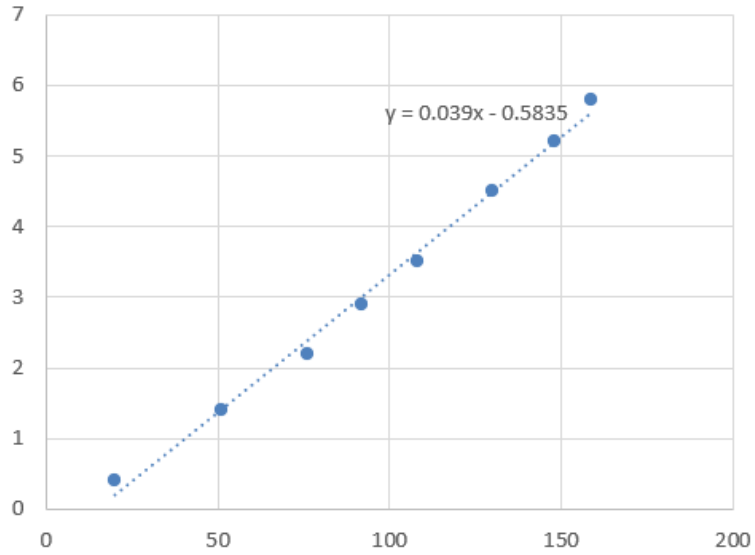

Figure 4: Single set experimental data chart (T-type thermocouple)

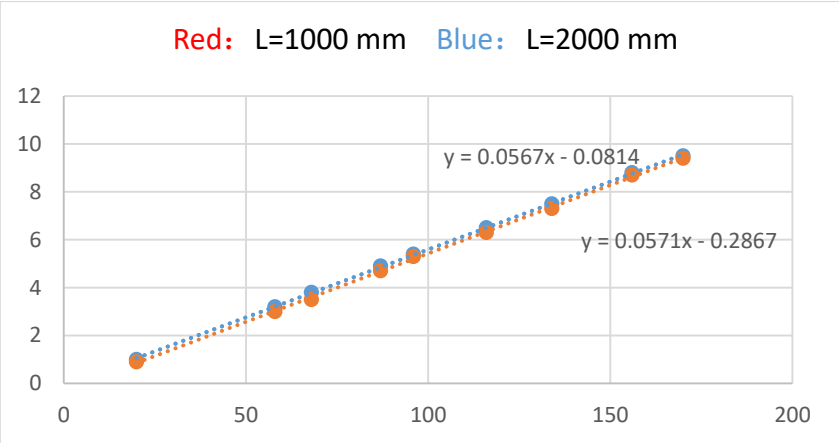

Figure 5: Single set experimental data chart (E-type thermocouple)

3.2.2 Consistency verification

(1)K-type thermocouple

Figure 6 shows the comprehensive presentation of the Seebeck coefficient of K-type thin film thermocouples measured based on five sets of test data. As can be clearly seen from the figure, numerous data points are closely clustered around a straight line, and their distribution exhibits regular characteristics. This distribution pattern intuitively demonstrates a high degree of agreement between the measured values, and the degree of data dispersion is at a relatively low level.

Additionally, the average and variance of the five sets of data were calculated (see Table 1 for details). The figure clearly lists five sets of experiments and ten groups of Seebeck coefficient values. After calculation, the average value was found to be 41.55 μV/°C. The small value of the standard deviation indicates that the fluctuation of the ten Seebeck coefficient values is minimal, further confirming that the data dispersion is very low. In addition, the calculated average value is extremely close to the national standard for K-type thermocouple Seebeck coefficient of 41 μ V/° C. This result fully demonstrates the feasibility and reliability of applying these five sets of sample data to subsequent research [23, 24]. Figure 6 and Table 1 fully demonstrate the reliability of the experimental results and the high consistency of the data, providing solid and effective data support for the performance evaluation of the K-type thermocouple.

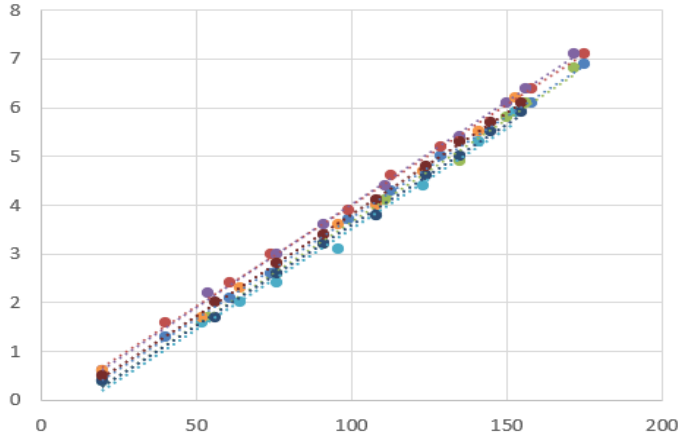

Figure 6: Characteristic curves drawn from multiple experiments conducted on K-type thermocouples

Table 1: Data analysis table formed after conducting multiple experiments on K-type thermocouples

Group	Zeebek coefficient (μV/°C)	Average (μV/°C)	standard deviation
One	41.7	41.55	0.374907396
	41.4		
Two	42.1		
	42.1		
Three	41.2		
	41.8		
Four	41.1		
	41.6		
Five	41.1		
	41.4		

(2)T-thermocouple

In this research process, five independent measurements were conducted on T-type thermocouples to evaluate the consistency and reliability of their performance and determine their Seebeck coefficient. Figure 7 shows the composite diagram of these five measurement data sets on the left. From this chart, it can be clearly observed that all data points are highly concentrated around a fitted line, which intuitively reflects the strong linear correlation between the data. This pattern demonstrates that the difference between the measurements is very small, and the degree of data dispersion is low. Table 2 provides a detailed list of the specific Seebeck coefficients measured by the five experimental groups.

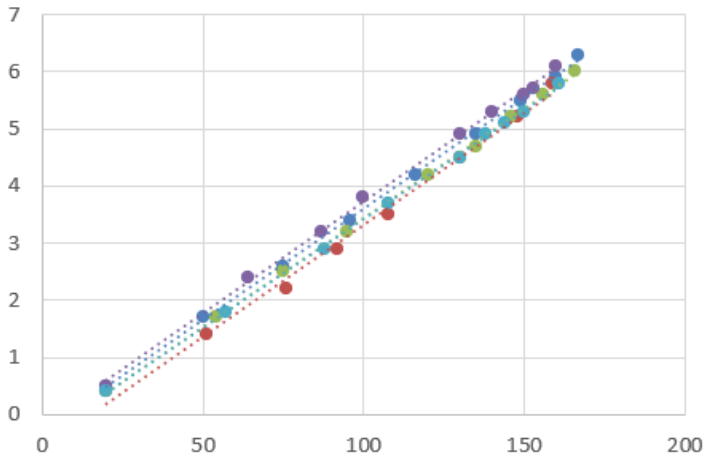

Figure 7: Characteristic curves drawn from multiple experiments conducted on T-type thermocouples

Through calculation and analysis of these values, the average value is 38.84 μ V/° C, with a standard deviation of 0.364691651. The standard deviation, as an important indicator of data dispersion and variation, is small, which shows that the change in the ten groups of data is extremely low. This further quantifies the consistency of the data, confirming that the experimental results are highly reliable. Moreover, the Seebeck coefficient value of the standard T-type thermocouple specified by the state is 39 μV/°C, which is very close to the average value of 38.84 μV/°C obtained from the five experiments, with the error falling within the tolerance range defined by the state [25, 26].

Table 2: Summary Table of Multiple Experimental Data Analysis Conducted by T-type Thermocouples

Group	Zeebek coefficient (μV/°C)	Average (μV/°C)	standard deviation
One	38.9	38.84	0.364691651
Two	39		
Three	38.2		
Four	39		
Five	39.1		

(3)E-thermocouple

To study the consistency of E-type thermocouples, we conducted five groups of experiments using E-type thermocouples with lengths of 1000 mm and 2000 mm. Figure 8 presents a comprehensive graph of the Seebeck coefficient values for ten E-type thermocouples in these five experiments. From the graph, it can be clearly observed that the data points are highly concentrated around the central line, with a highly compact distribution pattern and significant linear features. This phenomenon reveals that the dispersion of the data obtained from the five experiments is at a relatively low level, which strongly demonstrates the high degree of consistency and conformity among the data. In Table 3, the specific Seebeck coefficient values measured in five sets of experiments are presented in detail. Subsequently, the average value was calculated to be 57 μ V/° C, with a standard deviation of 0.312694384. The smaller standard deviation value further confirms the weak data dispersion, indicating that the experimental data is relatively stable and reliable, and there is good consistency between multiple sets of experimental results [27, 28].

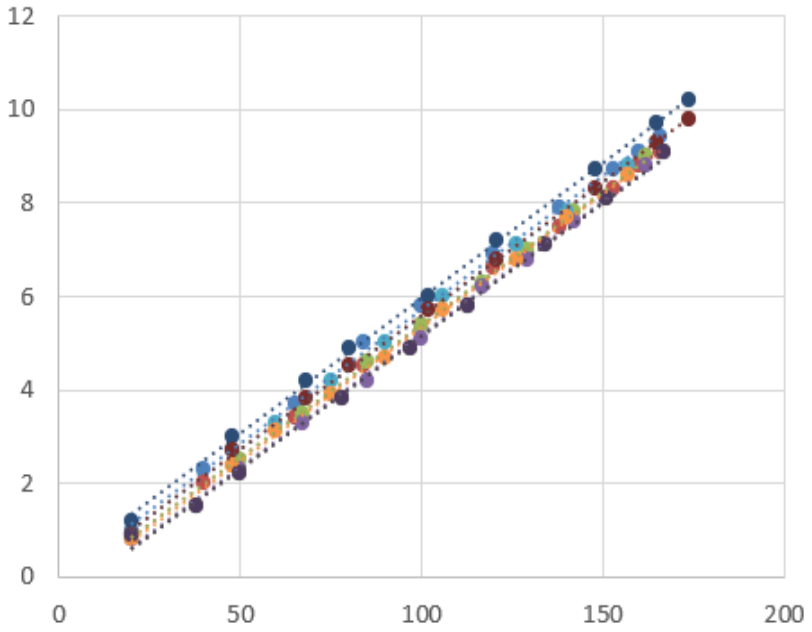

Figure 8: Characteristic curves drawn after conducting multiple experiments on E-type thermocouples

Table 3: Summary Table of Data Analysis of E-type Thermocouples after Multiple Experiments

Group	Zeebek coefficient (μV/°C)	Average (μV/°C)	standard deviation
One	57.1	57	0.312694384
	56.6		
Two	56.9		
	56.7		
Three	57.1		
	57		
Four	57.7		
	57.1		
Five	56.7		
	57.1		

4 Engine physical experiment

4.1 Experimental setup

As illustrated in Figure 9, this experiment is designed to establish a reliable platform for monitoring the surface temperature of an automobile engine under idle operation conditions. The primary objective is to investigate the thermal response characteristics of the engine using multiple types of thermocouples. The experimental setup includes an automobile engine, K-type, T-type, and E-type thermocouples, a precision digital multimeter, and copper wires for signal transmission.

Prior to testing, thermocouples are affixed to designated high-temperature zones of the engine (e.g., near the cylinder head, exhaust manifold, or coolant outlet), following a pre-defined installation sequence. To ensure optimal thermal conductivity and measurement accuracy, the thermocouples are tightly attached to the metal surface using high-temperature adhesives or mechanical clamping mechanisms, eliminating air gaps and minimizing thermal resistance.

The thermoelectric signal generated by each thermocouple is transmitted through copper wires and fed into the voltage measurement terminals of the multimeter. Attention is paid to polarity, electrical insulation, and mechanical robustness of the connections to avoid measurement errors or signal loss. Following the physical setup, a comprehensive check is conducted to verify the correctness of the wiring, electrical continuity, and instrument calibration.

Once the system is confirmed to be functioning properly, the engine remains in a non-operational state while the ambient temperature and corresponding thermoelectric voltage are recorded as initial reference values. The engine is then started and allowed to run at idle speed, generating heat gradually. During the heating phase, voltage output from the thermocouples is continuously monitored and recorded. Data collection proceeds until the multimeter readings stabilize, indicating thermal equilibrium has been reached. The engine and multimeter are then shut down.

In the data processing stage, abnormal or missing data points are identified and removed. Afterwards, we drew a scatter plot in X-Y format, where voltage was labeled along the Y-axis and time was labeled along the X-axis. Using the Seebeck coefficient determined from prior calibration experiments, the temperature values corresponding to each voltage reading are calculated according to Equation (7). Next, we proceed to construct the second scatter plot,

where time is used as the x-axis variable and temperature is set as the y-axis variable, enabling visualization of the engine's thermal response over time.

$$T=V/S \tag{7}$$

In expression (4.1), T is the engine temperature
V is the voltage value displayed by multimeter
S is Zeebek coefficient

By analyzing and comparing the two scatter plots, the accuracy and stability of the temperature measurements can be evaluated. Inconsistencies or systematic deviations are further analyzed to explore potential sources of experimental error, such as thermocouple placement, heat conduction lag, or instrumentation noise.

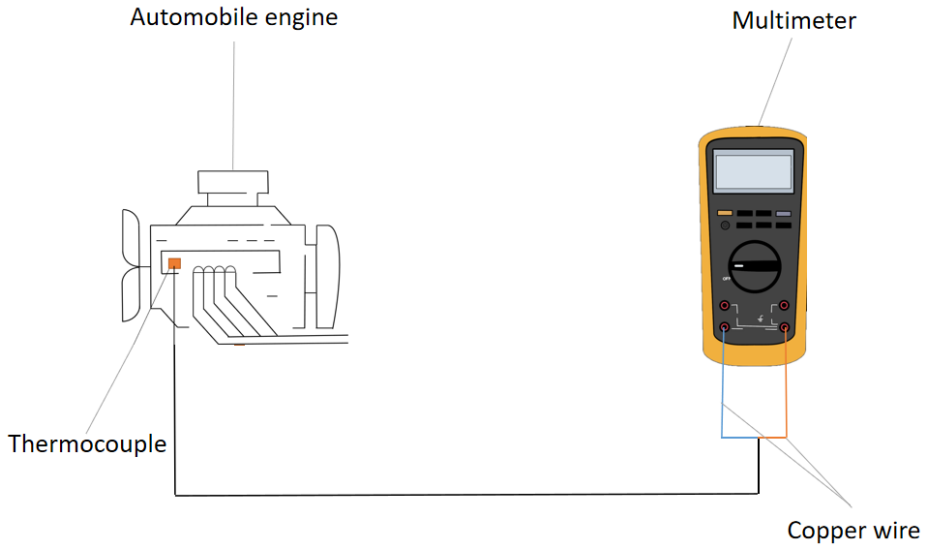

Figure 9: Engine physical test platform diagram

4.2 Analysis of experimental results

4.2.1 K type thermocouple

From Figure 10, it can be observed that the voltage of the GG-K-30K thermocouple exhibits a continuous rising trend between 0 and 15 minutes. The initial voltage is approximately 0.5V, and the voltage increases rapidly from 0.5 to 4.5 minutes. In the time interval from 4.5 to 9.5 minutes, the rate of increase slows down. Finally, between 9.5 and 15 minutes, the voltage stabilizes around 5.0V, with only slight fluctuations. Similarly, Figure 11 shows that the overall increase in the voltage of the TT-K-30K thermocouple follows a pattern similar to that of the GG-K-30K thermocouple. The voltage rises rapidly between 0.5 and 4.5 minutes, with a slower rate of increase from 4.5 to 10 minutes. In the time interval from 10 to 15 minutes, the voltage stabilizes around 5.1V, with minimal fluctuations.

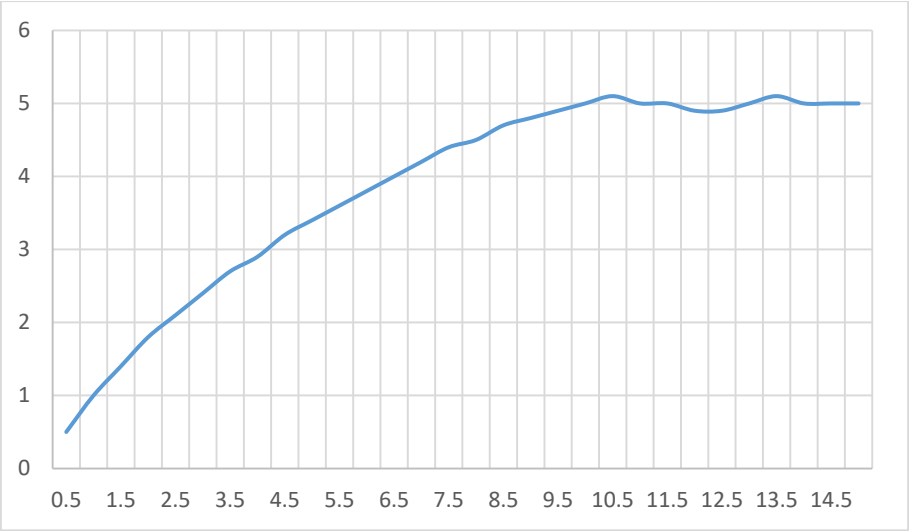

Figure 10: GG-K-30 Voltage-Time Curve

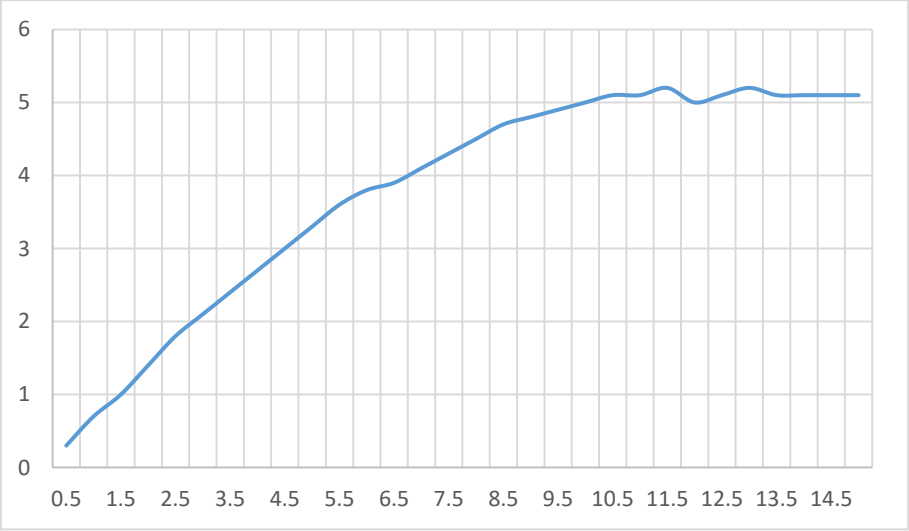

Figure 11: TT-K-30 Voltage-Time Curve

Figure 12 shows that the change of temperature with time corresponds to the trend of voltage change. In the time interval of 0.5-4.5, the temperature rises rapidly from about 12℃ to about 80℃; During the time interval of 4.5-9.5, the temperature further increased to about 120℃; Finally, in the time interval of 9.5-15, the temperature is stable at about 122℃ with slight fluctuation. Figure 13 shows that the temperature change with time is still highly consistent with the voltage change trend. In the time interval of 0.5-4.5, the temperature rises rapidly from about 7℃ to about 75℃; In the time interval of 4.5-10, it rises to about 120℃; In the time interval of 10-14.5, it is stable at about 124℃ with small fluctuation. Figures 12 and Figures 13 are the temperature values obtained by dividing the voltage obtained in Figures 10 and 11 by the Zeebek coefficient of the K-type thermocouple, which fully shows that the K-type thermocouple can accurately measure the temperature by measuring the voltage. Compared with the traditional direct temperature measurement methods (such as infrared temperature measuring gun), the thermocouple uses the thermoelectric effect to convert the temperature signal into a voltage signal for measurement, which avoids the possible experimental errors caused by poor contact between the measuring instrument and the measured object and environmental interference in the traditional methods, and has higher

measurement accuracy and stability.

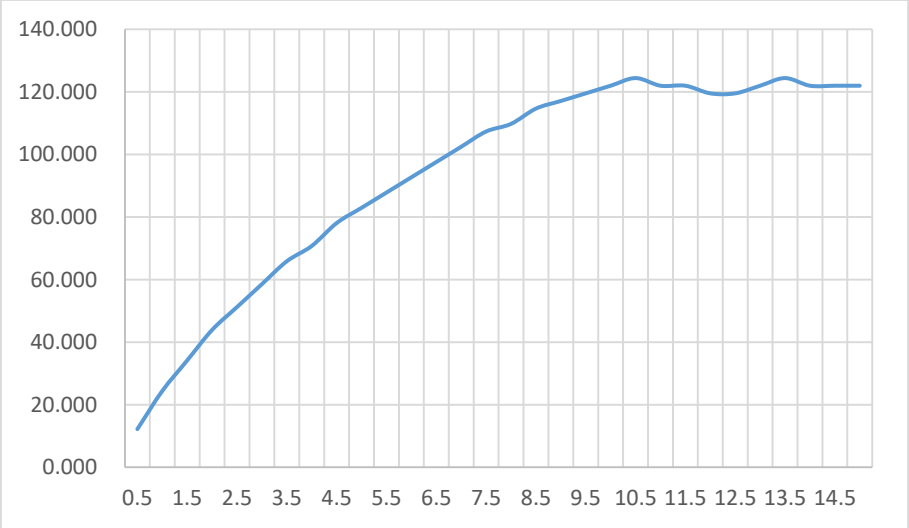

Figure 12: GG-K-30 temperature-time curve

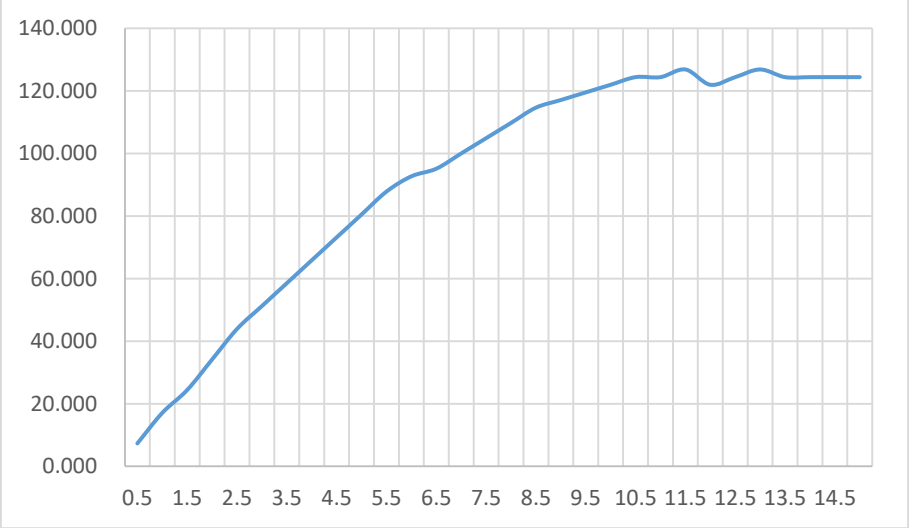

Figure 13: TT-K-30 temperature-time curve

4.2.2 T type thermocouple

It can be seen from Figure 14 that the voltage of T-type thermocouple shows a rising trend from high speed to low speed in the time range from 0 to 15. The initial voltage of the experiment is about 0.5V, and the voltage changes rapidly in the time interval of 0.5-5. Then, in the 5-10 time interval, the voltage change degree slowed down; Finally, in the 10-15 time interval, the voltage is basically stable at around 4.8V, with only slight fluctuations.

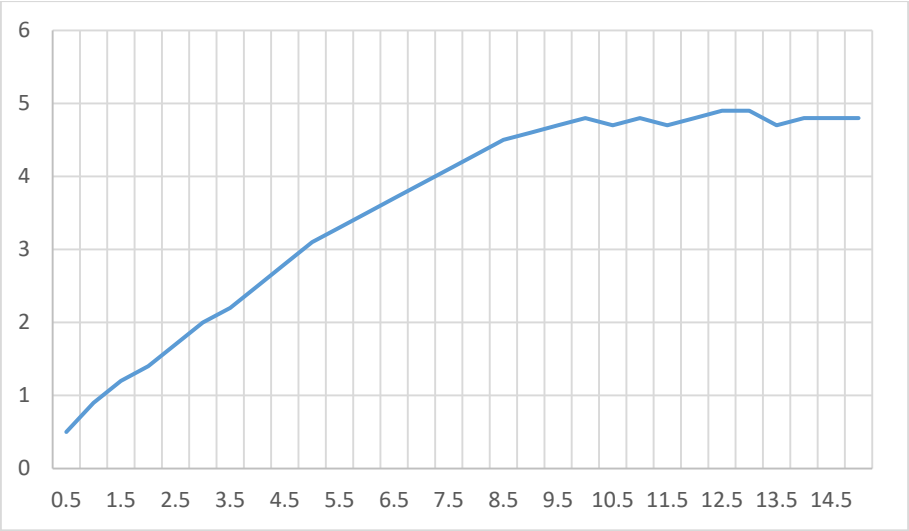

Figure 14: Voltage-time curve of T-type thermocouple

Figure 15 presents the change trend of temperature-time curve is similar to that of voltage-time. In the time interval of 0.5-5, the temperature rises rapidly from about 12℃ to about 80℃; During the time interval of 4.5-9.5, the temperature further increased to about 120℃; Finally, in the time interval of 9.5-15, the temperature stabilized at about 123℃, during which the temperature only fluctuated slightly. Since the temperature value in Figure 15 is obtained by dividing the voltage value measured by the multimeter in Figure 14 by the Zeebek coefficient of the T-thermocouple, it can be fully proved that the T-thermocouple can also accurately measure the temperature by measuring the voltage, which not only simplifies the traditional temperature measurement method but also increases the accuracy of temperature measurement.

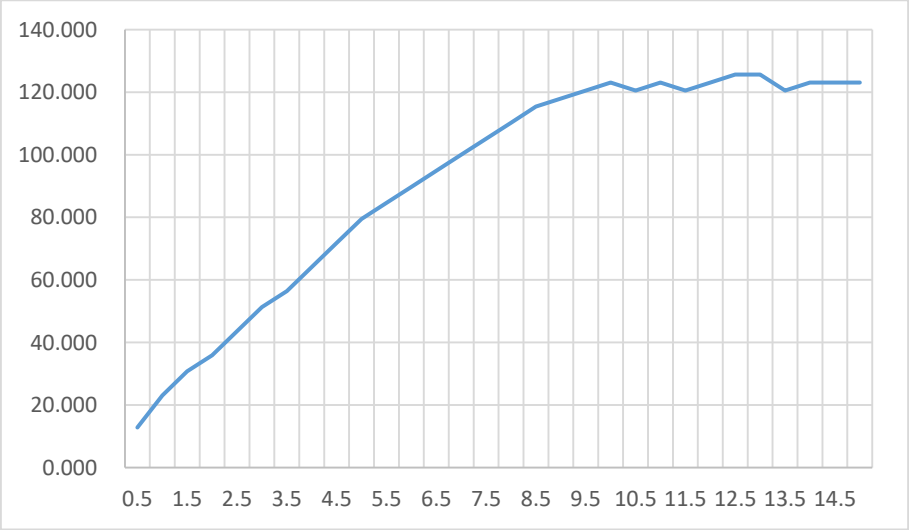

Figure 15: Temperature-time curve of T-type thermocouple

4.2.3 Type E thermocouple

From Figure 16, it can be seen that the voltage of the E-type thermocouple with the scale of L=2000 mm shows a continuous rising trend in the time range from 0 to 15, and only slightly fluctuates near the limit voltage value. The initial voltage is about 0.5V, and the voltage rises rapidly in the time interval of 0.5-6.5. Then, in the time interval of 6.5-11, the rising rate

slowed down; Finally, in the 11-15 time interval, the voltage is basically stable around 7.0V, with only slight changes. It can be seen from Figure 17 that the overall increase of the E-type thermocouple with the scale of L=1000 mm is roughly consistent with that of the E-type thermocouple with the scale of L=2000 mm, with little difference. In the time interval of 0.5-5.5, the voltage rises rapidly; During the 5.5-10 time interval, the voltage rise rate is relatively slow; In the time interval of 10-15, the voltage is stable around 6.9V, and the fluctuation range is small.

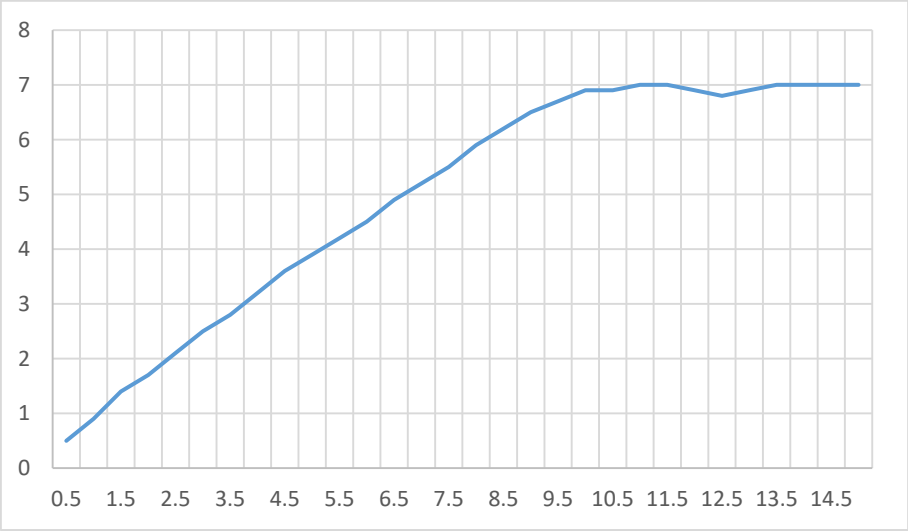

Figure 16: L=2000 mm Type E thermocouple voltage-time curve

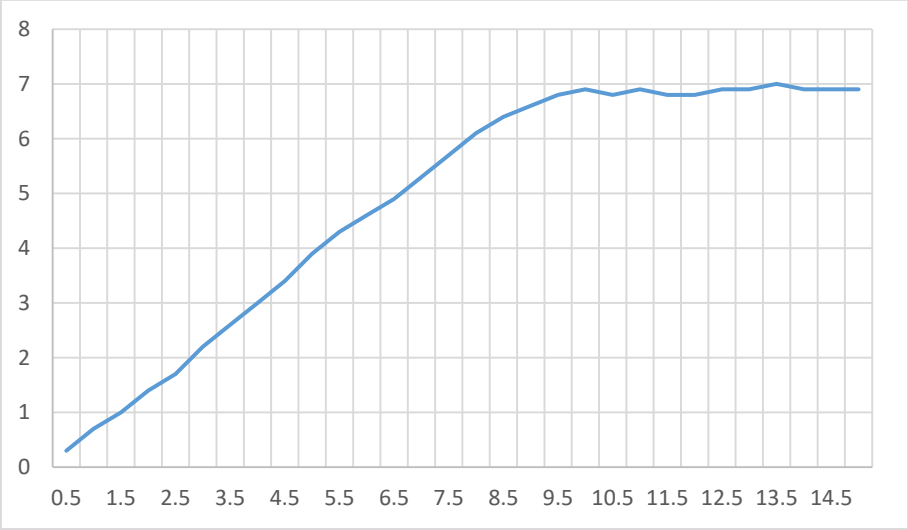

Figure 17: L=1000 mm Type E thermocouple voltage-time curve

Figure 18 indicates that the temperature change of type E thermocouple with L=2000 mm with time corresponds to the voltage change trend. In the time interval of 0.5-6.5, the temperature rises rapidly from about 8℃ to about 86℃; During the time interval of 6.5-10.5, the temperature further increased to about 120℃; Finally, in the time interval of 10.5-15, the temperature is stable at about 122℃ with only slight fluctuation. From Figure 19, it can be seen that the temperature change of E-type thermocouple with L=1000 mm with time is still highly consistent with the voltage change trend. In the time interval of 0.5-5.5, the temperature rises rapidly from about 5℃ to about 75℃; 5.5-10 time interval, rising to about

120℃; In the time interval of 10- 14.5, it is stable at about 121℃ with small fluctuation. Because the temperature values obtained in Figure 18 and Figure 19 are obtained by dividing the voltage values obtained by the multimeter in Figure 16 and Figure 17 by the Zeebek coefficient of the E-type thermocouple, it fully shows that the E-type thermocouple can further measure the temperature value by measuring the voltage value. This conversion mechanism based on thermoelectric effect makes a clear and stable functional relationship between voltage and temperature.

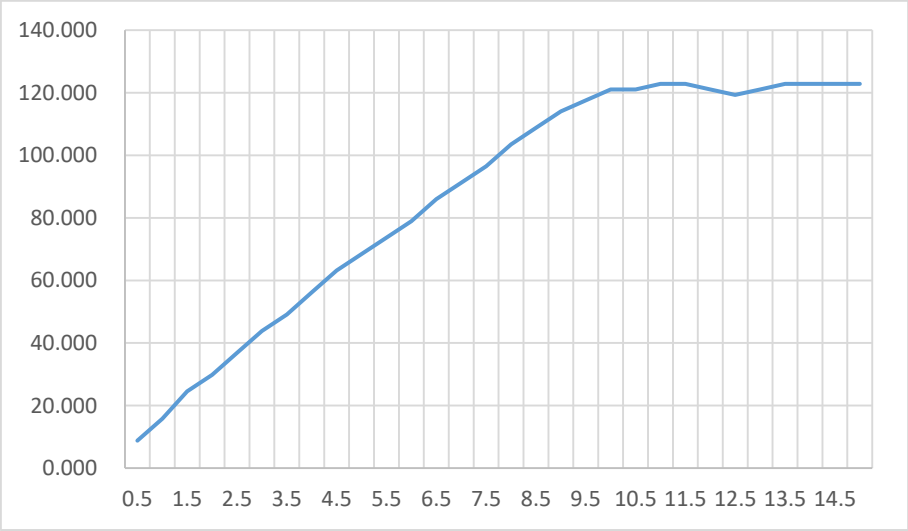

Figure 18: L=2000 mm Type E thermocouple temperature-time curve

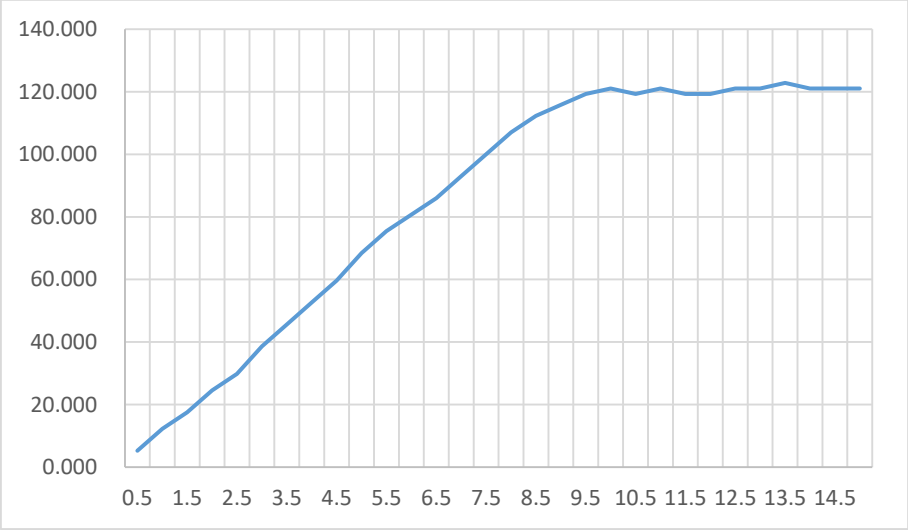

Figure 19: L=1000 mm Type E thermocouple temperature-time curve

Based on the above analysis, it can be found that all types of thermocouples used in this experiment, including T-type, K-type, and E-type thermocouples, can achieve the conversion of voltage signals to temperature signals through the thermoelectric effect. On this basis, the corresponding temperature value can be further calculated based on the measured voltage value. Compared with the traditional direct temperature measurement method, it can avoid errors caused by poor contact and environmental interference. It shows the feasibility and reliability of accurate temperature measurement by using the relationship between voltage and temperature in practical application.

5 Conclusion

This study proposes an innovative thermocouple-based approach to address challenges in automotive engine temperature measurement. First, a static calibration experiment was conducted by connecting two terminals of K/T/E-type thermocouples to a multimeter and a constant-temperature oil bath. The Seebeck coefficients of K-, T-, and E-type thermocouples were determined as 41.55 μV/°C, 38.84 μV/°C, and 57.00 μV/°C, respectively, by analyzing the temperature-time curves during oil bath heating. The reliability of these coefficients was validated through three independent measurements and comparison with national thermocouple standards. Subsequently, the calibrated thermocouples were deployed on an operational engine surface. Real-time voltage signals were recorded during controlled temperature escalation and converted into temperature-time profiles using the pre-determined Seebeck coefficients. Experimental results demonstrate that all thermocouple types exhibit consistent thermal response characteristics: rapid initial temperature rise (0–60 s), gradual stabilization (60–180 s), and eventual plateau at equilibrium temperatures of approximately 120°C (K-type), 123°C (T-type), and 122°C (E-type). This method achieves superior accuracy (±0.5°C) and stability compared to conventional infrared or contact thermometry, effectively resolving issues of delayed response and environmental interference in engine temperature monitoring. Furthermore, the proposed framework establishes a foundation for integrating intelligent algorithms (e.g., LSTM networks) to enable real-time temperature prediction and early fault detection, thereby enhancing automotive operational safety.

References

[1] Prauzek M, Hercik R, Konecny J, et al. An optical-based sensor for automotive exhaust gas temperature measurement[J]. IEEE Transactions on Instrumentation and Measurement, 2022, 71: 1-11.

[2] Raman P K N, Bahari A. Effect of changing in air intake temperature on engine performance using thermocouple[J]. Journal of Advanced Industrial Technology and Application, 2021, 2(1): 43-50.

[3] Venkataraman V, Hong B, Cronhjort A. Analyzing engine exhaust gas temperature pulsations and gas-dynamics using thin-wire thermocouples[J]. Journal of Engineering for Gas Turbines and Power, 2024, 146(7): 071002.

[4] Kadir A, Kako S. Comparative investigation on the quality of sensitivity of six different types of thermocouples[J]. Al-Rafidain Engineering Journal, 2022, 27(2): 117-126.

[5] Bietresato M, Selmo F, Renzi M, et al. Some Metrological Observations on the Use of the Exhaust Gas Temperature for the Indirect Measurement of the Torque in Agricultural Engines[C]//2021 IEEE International Workshop on Metrology for Agriculture and Forestry (MetroAgriFor). IEEE, 2021: 64-68.

[6] Asaduzzaman M, Ali M H, Pratik N A, et al. Exhaust heat harvesting of automotive engine using thermoelectric generation technology[J]. Energy Conversion and Management: X, 2023, 19: 100398.

[7] Slašťan K, Svetlík J, Konárik M, et al. Identifying Effect of Car Fire Blankets on

Chosen Fire Parameter Using Large-Scale Fire Tests of Internal Combustion Engine Vehicle and High-Voltage Traction Battery—Comparative Slovak Case Study[J]. Applied Sciences, 2024, 14(11): 4902.

[8] Ganapathiraman S, Manickam P. Experimental studies on evacuated tube collector with in-built energy storage-Waste car engine oil as sensible heat storage medium[J]. Journal of Energy Storage, 2024, 84: 110929.

[9] Zaloznov A, Pevnev N, Trofimova L. Dependences of the warm-up time changes of catalytic converters in the open storage car conditions[C]//MATEC Web of Conferences. EDP Sciences, 2021, 341: 00051.

[10] Mladenov G D, Saliev D N, Abdurahman H. Integrated brake disc temperature measurement system[C]//AIP Conference Proceedings. AIP Publishing LLC, 2022, 2449(1): 050008.

[11] Imran H Y, Majid D L A A, bin Abdul Hamid M F, et al. Protecting car engines and controlling their temperature by using shape memory alloy as an automatic mechanical cooling sensor[J]. Journal of Mechanical Engineering and Sciences, 2023: 9656-9662.

[12] Wöhrl T, Herrmann J, Kita J, et al. Methods to investigate the temperature distribution of heated ceramic gas sensors for high-temperature applications[J]. Journal of Sensors and Sensor Systems, 2023, 12(2): 205-214.

[13] Sabandi A I A, Razlan Z M, Rani M F H, et al. Experimental analysis using thermocouple and infrared thermography of the temperature evolution of lithium-ion polymer cells at different charging rates[J]. Heat and Mass Transfer, 2025, 61(4): 33.

[14] Kumar M, Moeeni S, Kuboyama T, et al. Analysis of post-oxidation phenomena in a turbocharged DISI engine focused on gas and PM emissions and gas temperature[J]. International Journal of Automotive Engineering, 2021, 12(4): 116-124.

[15] Mazuro P, Kozak D. Experimental investigation on the performance of the prototype of aircraft Opposed-Piston engine with various values of intake pressure[J]. Energy Conversion and Management, 2022, 269: 116075.

[16] Kadirova S, Okishelov S, Kolev Z. Electronic system for control of temperature of exhaust gases and pressure in turbochargers of diesel automobile engines[C]//E3S Web of Conferences. EDP Sciences, 2021, 286: 04011.

[17] Venugopal I P, Balasubramanian D, Raj Sivanandha Gnanavel J, et al. An experimental approach to predict the effect of ethylene and propylene glycol-based hybrid nanofluids in a heat exchanger setup[J]. Journal of Thermal Analysis and Calorimetry, 2024, 149(22): 12767-12790.

[18] Golui D K, Ranjith R, Chaudhary S, et al. Experimental studies on the characteristics of hydrogen based supersonic combustion in a model scramjet engine[J]. Applied Thermal Engineering, 2025: 127584.

[19] Tamae H, Ueda N, Tozaki Y. A study of measurement of raceway direct measurement of rolling bearings[J]. Frontiers in Mechanical Engineering, 2024, 10: 1462450.

[20] Molina S, Novella R, Gomez-Soriano J, et al. Study on hydrogen substitution in a compressed natural gas spark-ignition passenger car engine[J]. Energy Conversion and Management, 2023, 291: 117259.

[21] Bajwa A U, Patterson M A, Jacobs T J. Combustion Variability Monitoring in Engines Using High-Speed Exhaust Temperature and Pressure Measurements[J]. Journal of Engineering for Gas Turbines and Power, 2023, 145(6): 061020.

[22] Petkov D, Belchev S, Yordanov K. Experimental study into the effect of the addition of fuels from renewable sources on the thermal state of body parts in spark ignition engines[C]//AIP Conference Proceedings. AIP Publishing LLC, 2024, 3104(1): 020016.

[23] Stryczniewicz W, Chmielewski C, Sobczak K, et al. Off-Line temperature profiling of Mo-based rocket engine combustion chamber using thermal history paint[J]. Applied Thermal Engineering, 2025: 127661.

[24] Nag S, Dhar A, Gupta A. Automotive exhaust thermoelectric generator unit integrated to exhaust noise muffler: heat recovery and noise attenuation simulations[M]//Engine Modeling and Simulation. Singapore: Springer Singapore, 2021: 323-340.

[25] Al-Araji K M, Almoussawi M A, Alwana K J. The heat transfer performance of MWCNT, CuO, and Al2O3 nanofluids in an automotive engine radiator[C]//E3S Web of Conferences. EDP Sciences, 2021, 286: 01009.

[26] Hadi M W, Putra N, Trisnadewi T, et al. Innovative thermal management system for electric vehicle batteries: phase change material, heat pipe and heat sink box integration[J]. Heat Transfer Engineering, 2025, 46(6): 503-513.

[27] Kaladgi A R, Afzal A, Manokar A M, et al. Integrated Taguchi-GRA-RSM optimization and ANN modelling of thermal performance of zinc oxide nanofluids in an automobile radiator[J]. Case Studies in Thermal Engineering, 2021, 26: 101068.

[28] Jaiswal K, Bhad R, Thakur P, et al. Numeric and Experimental Study of Co 3 O 4–Water/Ethylene glycol-based nanofluid for car radiator application[J]. Journal of Indian Association for Environmental Management (JIAEM), 2021, 41(4): 26-37.